BMC Plant Biology

RESEARCH

Open Access

# Dual roles of pear *EARLY FLOWERING 4 -like* genes in regulating flowering and leaf senescence

Zhe Liu[1,2†], Weijuan Liu[2†], Qiong Wu[2†], Zhihua Xie[2], Kaijie Qi[2], Shaoling Zhang[2], Juyou Wu[2] and Peng Wang[2*]

## Abstract

**Background** Flowering is a critical agronomic trait in fruit tree cultivation, essential for sexual reproduction and fruit yield. Circadian clock system, governing processes such as flowering, growth, and hormone signaling, plays a key role in plant adaptability. While some clock-related genes influencing pear flowering have been studied, the role of the PbELF4 (EARLY FLOWERING 4) family remains largely unexplored.

**Results** In this study, we identified five *ELF4* homologous genes within the pear (*Pyrus bretschneideri*) genome. Phylogenetic analysis delineated two distinct groups within the *PbELF4* genes, with *PbELF4a* and *PbELF4b* clustering with *AtELF4*. Expression profiling across various pear tissues revealed diverse expression patterns. Diurnal rhythms of *PbELF4* genes were discernible in pear leaves, suggesting potential regulatory roles. Ectopic overexpression of *PbELF4a* and *PbELF4b* in Arabidopsis significantly delayed flowering and suppressed the expression of flowering-related genes. Additionally, *PbELF4b* overexpression induced premature leaf senescence, evidenced by reduced chlorophyll content and increased expression of senescence-associated genes. Nuclear localization of PbELF4a and PbELF4b proteins was observed, and interaction assays revealed that PbELF4a interacted with PbELF3α.

**Conclusions** These findings underscore the conserved function of *PbELF4a* and *PbELF4b* as negative regulators of flowering time, with *PbELF4b* also demonstrating a positive role in leaf senescence.

**Keywords** *Pyrus bretschneideri*, ELF4, Flowering time, Leaf senescence, Functional analysis

## Background

Flowering represents a pivotal transition from vegetative growth to reproductive growth in higher plants, bearing immense significance for plant growth and agricultural development. Therefore, understanding the regulation and molecular mechanisms of flowering is crucial. The initiation of flowering in plants is intricately controlled by complex regulatory networks that encompass factors such as photoperiod, vernalization, ambient temperature, gibberellin, age, and autonomous pathways [1, 2]. To synchronize flowering time with environmental cues, plants have evolved precise mechanisms involving an array of genes within the circadian clock system and photoperiod pathway [3, 4]. In *Arabidopsis thaliana* (Arabidopsis), the circadian clock oscillator operates through feedback loops involving in several genes, including *CIRCADIAN CLOCK ASSOCIATED 1* (*CCA1*)/ *LONG ELONGATED HYPOCOTYL* (*LHY*), *PSEUDO-RESPONSE REGULATORs* (*PRRs*), *LUX ARRHYTHMO* (*LUX*), *EARLY FLOWERING 3* (*ELF3*), and *ELF4* [5]. *ELF4*, among the

†Zhe Liu, Weijuan Liu and Qiong Wu contributed equally to this work.

*Correspondence:
Peng Wang
wangpeng@njau.edu.cn
[1] School of Pharmacy, Changzhi Medical College, Changzhi 046000, China
[2] Sanya Institute of Nanjing Agricultural University, State Key Laboratory of Crop Genetics & Germplasm Enhancement and Utilization, Jiangsu Key Laboratory for Horticultural Crop Breeding, College of Horticulture, Nanjing Agricultural University, Jiangsu 210095, China

core components of the oscillator, participates in photoperiodic perception, circadian regulation, and negative regulation of flowering in Arabidopsis [6].

The ELF4 family constitutes a group unique to the plant kingdom, which is characterized by the presence of a highly conserved DUF1313 domain. In Arabidopsis, this family comprises *ELF4* and four homologs (*EFL1*–*EFL4*) [6–8], and extensive research has been undertaken over the past two decades to elucidate the functions and molecular mechanisms of *ELF4* genes. ELF4 forms an evening complex (EC) together with ELF3 and LUX [9], and *elf3*, *elf4*, and *lux* mutants exhibit similar early-flowering phenotypes, with the expression of these three genes peaking at dusk [6, 10–12]. The EC integrates environmental and endogenous signals to regulate the expression of key genes involved in the circadian clock, photosynthesis, phytohormone signaling, and growth [13]. *GIGANTEA* (*GI*) is a crucial circadian clock gene implicated in flowering time regulation. Genetic studies have shown that GI is epistatic to ELF4 in flowering time regulation, as *gi elf4* double mutants exhibit flowering phenotypes similar to *gi* single mutants under long- and short-day conditions [14]. Additionally, *ELF4* regulates photoperiodic flowering by modulating the nuclear distribution of GI and its binding to the promoter of *CONSTANT (CO)* [15]. In Arabidopsis, overexpression of *EFL1* and *EFL3*, which are homologous genes of *ELF4*, delays flowering in the *elf4* mutant. They also suppress the expression of flowering-related genes *CO* and *FLOWERING LOCUS T* (*FT*) [8].

ELF4 family members in other species also play roles in controlling flowering. For instance, *DNE*, an ortholog of *AtELF4* in *Pisum sativum*, inhibits flowering under short-day conditions [16]. In *Dimocarpus longan* L., *ELF4* is a pivotal candidate gene associated with the flowering trait, as identified through high-throughput RNA sequencing. Furthermore, *DlELF4-1* and *DlELF4-2*, when expressed in Arabidopsis, have been found to delay flowering [17, 18]. *ELF4* genes such as *DhEFL2*, *DhEFL3* and *DhEFL4* in *Doritaenopsis* hybrid are implicated in the control of flowering processes [19]. The adaptation of *Glycine max* (soybean), a species native to temperate regions, to low-latitude environments is attributed to mutations at the *J* locus [20]. *J* is the homologue of *ELF3* gene and a component of the EC. The mutations of *LUX* homologous genes, another component of the EC, significantly affected soybean flowering and photoperiod sensitivity [21]. Meanwhile, overexpression of *GmELF4* delayed flowering in Arabidopsis [22]. As a core regulator, the EC plays a crucial role in determining the planting distribution and yield of soybean across different latitudes.

In addition to their role in flowering regulation, *ELF4* genes exhibit pleiotropic effects encompassing seedling de-etiolation, temperature response, stress resistance, and leaf senescence [23–26]. Leaf senescence, an integral aspect of the plant life cycle, is intricately linked to the reallocation of nutrients to ensure successful reproductive development and environmental adaptation [27, 28]. In the elucidated genetic network, the expression of numerous *SENESCENCE-ASSOCIATED GENES* (*SAGs*), including a substantial number of NAM/ATAF/CUC (NAC) transcription factor family genes in Arabidopsis, undergoes modulation [29, 30]. Furthermore, emerging evidences suggest that certain circadian clock genes play roles in leaf senescence [31, 32].

In Arabidopsis, CCA1, a core component of the circadian clock, regulates leaf senescence by directly activating Golden2-like transcription factors (GLK2) while inhibiting the expression of *ORESARA 1* (ORE1, also known as ANAC092) [33]. Unlike *CCA1*, which exerts a negative regulatory influence on senescence, PRR9 combines with the *ORE1* promoter to enhance its expression, thereby positively regulating leaf senescence [34]. Additionally, *elf3*, *elf4*, and *lux* mutants exhibit early leaf-senescence phenotypes under long-day conditions and demonstrate responsiveness to jasmonate (JA) induction. EC has been shown to regulate JA-induced leaf senescence by inhibiting *MYC2* transcription, thereby modulating downstream *SAGs* [26]. *ELF3* suppresses dark-induced leaf senescence through the action of *PIF4/PIF5* in an EC-independent manner [35]. Recently, ELF4 has been found to hinder the binding of GI to the *ORE1* promoter [36]. However, the molecular mechanisms underlying the interplay between the circadian clock system and leaf senescence, as well as the key genes involved, remain to be fully discovered and elucidated.

Pear (*Pyrus*) is a renowned perennial fruit crop within the Rosaceae family, with significant economic benefits. Timely flowering is imperative for fruit yield and quality in pear cultivation, while leaf senescence serves as a critical factor directly influencing fruit development. Although EC was identified in pear with similar components ELF3 and LUX [37], the ELF4 family members and their functions in pear remained unexplored. In this study, we aimed to fill this gap by identifying five *PbELF4* genes from the pear genome [38] and further analyzing their phylogenetic relationships, conserved domains, gene structures, and expression patterns. Additionally, we isolated *PbELF4a* and *PbELF4b* genes and investigated their potential functions through ectopic overexpression in Arabidopsis. Our research shed light on the potential roles of *ELF4* genes in governing the growth and reproductive stages of pear, providing valuable insights into the molecular processes underlying pear development.

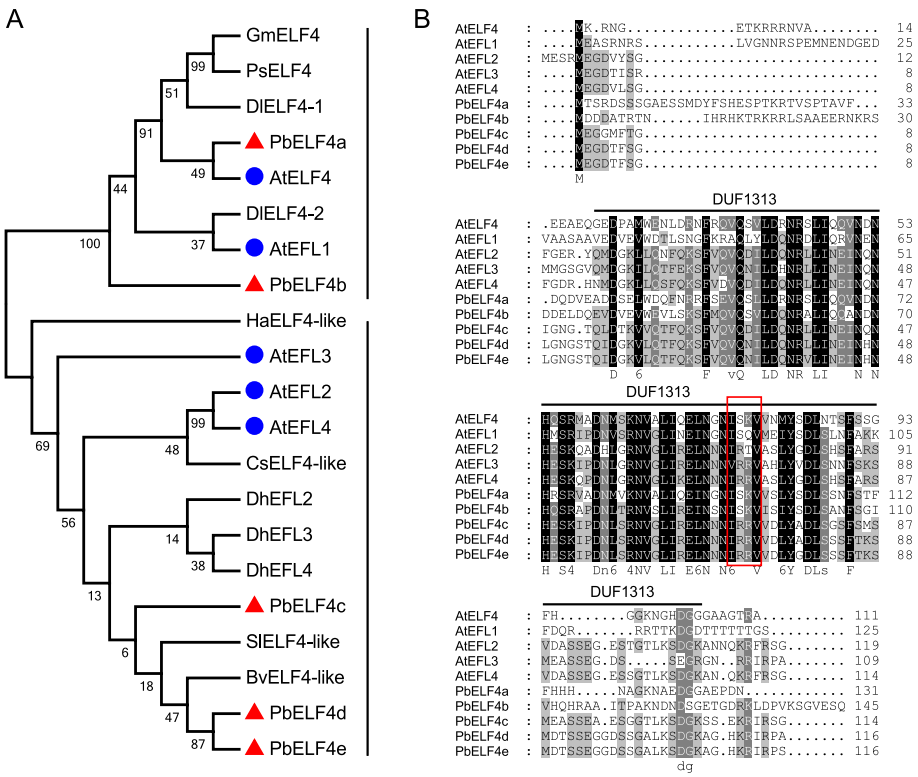


**Fig. 1** Phylogenetic relationship analysis and multiple sequence alignment of PbELF4 proteins. **A** Maximum likelihood phylogenetic tree showing the evolutionary relationships among ELF4/ELF4-like proteins from pear and other species. The red triangles and blue dots indicate members in pear and Arabidopsis, respectively. **B** Amino acid sequence alignment of ELF4/ELF4-like proteins from pear and Arabidopsis. The DUF1313 domain is marked with a black horizontal line, and the red box denotes four conserved amino acid residues

## Results

### Identification and characterization of PbELF4 genes in pear

In Arabidopsis, the ELF4 family encompasses five members, namely *ELF4* and *EFL1* to *EFL4* [7]. To identify homologous genes in pear (*P. bretschneideri*) genome, we utilized the five ELF4 and EFL protein sequences from Arabidopsis as queries in a BLASTP search. Consequently, we obtained five *ELF4-like* candidate genes, designated as *PbELF4a* to *PbELF4e*. To elucidate the evolutionary relationship of *ELF4* genes between pear and other species, a maximum likelihood tree was constructed using ELF4/ELF4-like protein sequences from nine reported species and pear. The tree delineated all ELF4 members into two distinct groups (Fig. 1A). Specifically, PbELF4a and PbELF4b clustered together with AtELF4 and AtEFL1, while PbELF4c, PbELF4d, and PbELF4e grouped with AtEFL2, AtEFL3, and AtEFL4 in another group. *PbELF4a*, closest to AtELF4, encoded a protein consisting of 131 amino acids with a calculated molecular mass of 14.698 kDa (Fig. 1A and Table S1). Among the five pear proteins, PbELF4b possessed the longest amino acid sequence, encoding a 16.434 kDa protein comprising 145 amino acids (Table S1). The theoretical isoelectric points (pI) of pear proteins ranged from 4.82 to 6.83. Furthermore, the five *PbELF4* genes were mapped to chromosomes 1, 2, 9, 11, and 15.

Multiple sequence alignment revealed that PbELF4-like proteins possessed the central conserved region known as the DUF1313 domain, indicating their classification within the ELF4 family (Fig. 1B). Sequence analysis demonstrated that compared to other members of Arabidopsis, PbELF4a and PbELF4b exhibited higher identity with AtELF4, at 47.37% and 38.62%, respectively. A previous study categorized DUF1313 predictive proteins from various species into three types based on four amino acid residues: IARV-type, I(S/T/F)(K/R)V-type, and IRRV-type [39]. Notably, PbELF4a and PbELF4b shared the same residues (ISKV) as AtELF4, while PbELF4c, PbELF4d, and PbELF4e were classified as IRRV-type, representing the largest subtype containing putative genes (Fig. 1B). Furthermore, NCBI Batch CD-Search reaffirmed the presence of a typical DUF1313 domain in all five PbELF4 proteins (Fig. 2A). Gene structure analysis revealed that all *PbELF4* genes comprised a single exon without any introns, consistent with the structure of *AtELF4* genes (Fig. 2B).

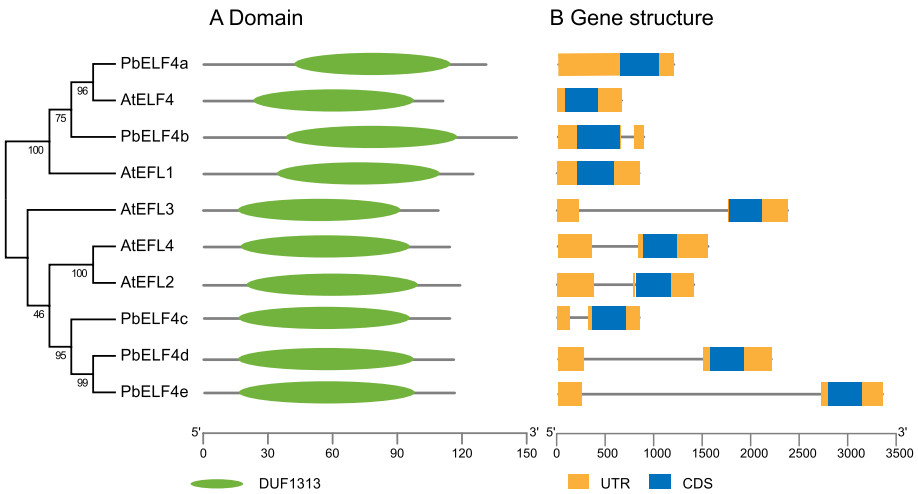


**Fig. 2** Conserved domain and gene structure analysis of ELF4/ELF4-like members in pear and Arabidopsis. **A** The DUF1313 domain, represented by a green oval, was identified using the Conserved Domain Database. **B** Gene structure diagram showing untranslated 5′- and 3′-regions (UTRs) in orange boxes, exons in blue boxes, and introns in gray lines

During evolution, gene duplication plays a crucial role in gene family expansion and functional diversification. In the PbELF4 family, we observed two paralogous gene pairs derived from dispersed duplication (DSD), along with three pairs derived from whole-genome duplication (WGD) (Table S2). Ks values, commonly used to estimate evolutionary time, provide insights into the timing of duplication events in the pear genome. Specifically, two major duplication events have been identified: the ancient WGD (Ks = 1.5–1.8) and the recent WGD (Ks = 0.15–0.3) [38]. The Ks value between *PbELF4a* and *PbELF4b* was approximately 1.035, suggesting that this pair stemmed from an ancient duplication event. However, *PbELF4e* and *PbELF4d* exhibited a lower Ks value, indicating a more recent duplication event (Table S2).

### Expression analysis of PbELF4 genes

To elucidate the potential biological functions of *PbELF4* genes in pear growth and development, we investigated the expression patterns of five *PbELF4* genes across various tissues. The expression profiles of *PbELF4* genes were analyzed using transcripts per kilobase million (TPM) values of 24 pear tissues obtained from published transcriptomic information in Pear Expression Database [40]. These tissues included four seedling tissues, four adult tissues, six flower organ tissues, mixed samples of pericarp and flesh at five fruit developmental stages, and five fruit tissues at 145 days after full bloom (DAF).

With the exception of *PbELF4a*, which was not detected in stamen, all five *PbELF4* genes exhibited expression across all tissues and fruit developmental stages, albeit with different expression patterns (Fig. 3A). Among the 14 pear tissues examined at the seedling, adult, and floral organ stages, *PbELF4a* showed the highest expression levels in leaf buds, followed by that in flower stalks, juvenile stems, and flower buds. Interestingly, *PbELF4a* transcript levels were higher in the early stages of fruit development and decreased gradually with fruit maturation. Conversely, *PbELF4b* displayed higher expression in stamen compared to that in the other 13 tissues, with expression levels increasing gradually during fruit development. *PbELF4c* exhibited high expression levels across most tissues, particularly in stems and the four fruit tissues at 145 DAF. *PbELF4d* showed extremely low expression levels in seeds but very high expression levels in the mixed samples of fruit tissues at 85 DAF. In contrast, *PbELF4e* displayed relatively low expression levels during fruit developmental stages but significantly higher expression levels across flower organs. These findings suggest that *PbELF4* genes are involved in multiple stages of pear development and may play diverse roles in regulating various developmental processes.

To examine the diurnal rhythm patterns of *PbELF4* genes, we assessed their expression levels over a 24-hour period under three different conditions. The results revealed that *PbELF4* genes have distinct diurnal rhythms and respond to photoperiodic changes. Under 12 h light/12 h dark conditions, the expression of *PbELF4a* peaked at dawn (zeitgeber time 1; ZT1), followed by a sharp decrease, with a gradual increase after ZT5. In contrast, *PbELF4b* exhibited an additional expression peak at night (ZT17). The expression of *PbELF4c* and *PbELF4e* initially decreased during daytime, followed by an increase at night, with peak expression levels occurring around dawn (Fig. 3B). Under long- and short-day conditions, *PbELF4* genes showed different expression patterns

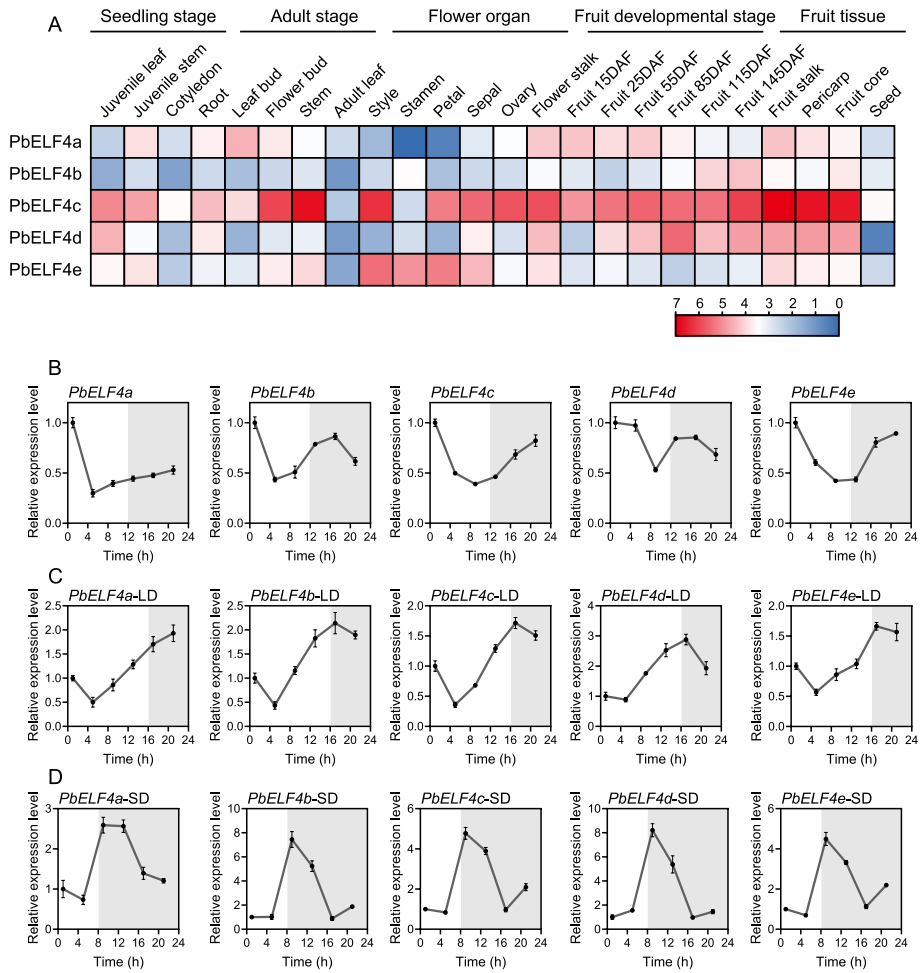


**Fig. 3** Expression analysis of *PbELF4* genes. (**A**) Expression profiles of *PbELF4* genes in various pear tissues, including four seedling tissues (juvenile leaf, juvenile stem, cotyledon, and root), four adult tissues (leaf bud, flower bud, stem, and adult leaf), six flower organ tissues (style, stamen, petal, sepal, ovary, and flower stalk), mixed samples of pericarp and flesh at five fruit developmental stages [15 days after full bloom (DAF) to 115 DAF], and five fruit tissues at 145 DAF (flesh, fruit stalk, pericarp, fruit core, and seed). Expression levels are shown as $\log_2$ (TPM +1) values of each gene, with the color gradient indicating expression intensity. The scale bars from red to blue indicate the expression levels from high to low. **B**, **C**, **D** Diurnal expression patterns of *PbELF4* genes in pear seedlings. **B** Expression patterns under 12 h light/12 h dark conditions. **C** Expression patterns under long-day conditions (LD, 16 h light/8 h dark). **D** Expression patterns under short-day conditions (SD, 8 h light/16 h dark). The light was turned on for 1 hour to start sampling, each with an interval of 4 hours. White and grey areas indicate light and darkness, respectively. The expression of each gene in sample 1 was set to "1." *PbUBQ* was used as an internal control. Data are presented as means ± standard deviation (SD) ($n = 3$)

with significant changes in peak time (Fig. 3C and 3D). For example, *PbELF4b* exhibited higher expression at night (ZT17) under long-day conditions, while its expression peaked during the afternoon (ZT9) under short-day conditions.

### Overexpression of PbELF4a and PbELF4b delayed flowering in Arabidopsis

To explore the functions of PbELF4-like proteins, PbELF4a and PbELF4b, which displayed higher homology to AtELF4, were specifically targeted for functional analysis. The full-length coding sequences of these two genes were cloned into vectors carrying the CaMV 35S promoter and subsequently transformed into Arabidopsis plants (Col-0), generating heterologous overexpression (OE) transgenic lines. All transgenic lines exhibited significant delayed flowering phenotypes under long-day conditions (16 h light/8 h dark) (Fig. 4A). Quantitative PCR analysis confirmed the expression of *PbELF4a* and *PbELF4b* in their respective transgenic lines compared to those in vector control plants (Fig. 4B and Fig. S1).

In comparison to the average flowering time of vector control plants, PbELF4a-OE1 and OE2 lines exhibited delayed flowering by 4.44 and 8.84 days, respectively

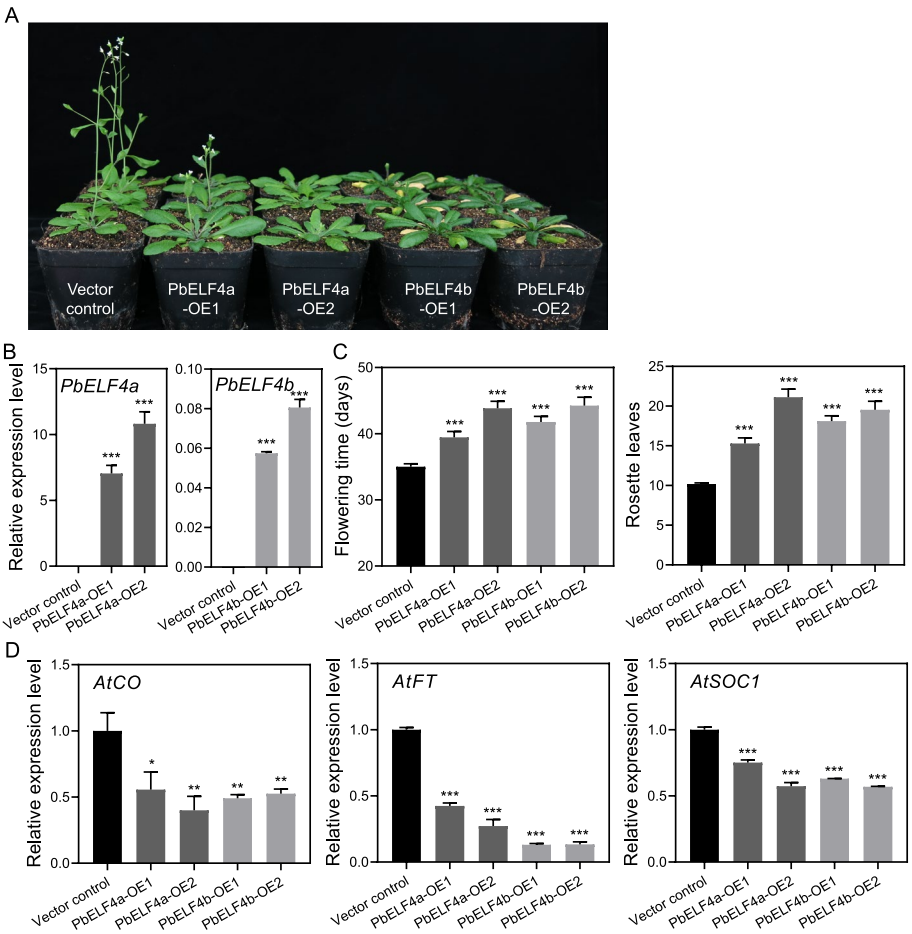


**Fig. 4** Overexpression of *PbELF4a* and *PbELF4b* delayed flowering in Arabidopsis plants. **A** Flowering phenotypes of vector control plants, PbELF4a-OE, and PbELF4b-OE transgenic lines grown under long-day conditions (16 h light/8 h dark) for 38 days. The number of rosette leaves of vector control plants was 10, while PbELF4a-OE1 lines was 13 and 14. The first flower of PbELF4a-OE2, PbELF4b-OE1, and PbELF4b-OE2 did not open; hence, the number of rosette leaves was not counted. **B** Quantitative RT-PCR analysis of *PbELF4a* and *PbELF4b* expression in control plants and transgenic lines. Data are presented as means ± SD ($n = 3$). **C** Days to first flowering and number of rosette leaves at first flowering of control plants and transgenic lines. Data are presented as means ± standard error of the mean (SEM) ($n \geq 24$). **D** Expression levels of flowering-related genes in 10-day-old seedlings from control plants and transgenic lines. The expression of each gene in control plants was normalized to a value of "1." *AtACT* served as the internal control for gene expression analysis. Data are presented as means ± SD ($n = 3$). Statistical significance was determined using Student's *t*-tests compared to the vector control plants. * Indicates $P < 0.05$, ** indicates $P < 0.01$, and *** indicates $P < 0.001$

(Fig. 4C). Similarly, compared to vector control plants, PbELF4b-OE1 and OE2 lines displayed delayed flowering by 6–9 days. Additionally, the number of rosette leaves at the onset of flowering, an important developmental indicator, was higher in transgenic lines overexpressing *PbELF4a* and *PbELF4b* compared to that in vector control plants. To elucidate the potential molecular mechanisms underlying the delayed flowering phenotype induced by *PbELF4* overexpression, we examined the expression levels of flowering-related endogenous genes in transgenic lines and control plants (Fig. 4D). The expression of *AtCO*, a hub gene in the photoperiod pathway regulating flowering, was significantly suppressed in Arabidopsis plants overexpressing *PbELF4a* and *PbELF4b*. Moreover, the expression levels of flowering integration factors *AtFT* and *AtSOC1* were downregulated in transgenic lines. These findings suggest that both *PbELF4a* and *PbELF4b* may contribute to the delayed flowering phenotype by modulating the expression of key flowering regulatory genes.

### Overexpression of PbELF4b promotes leaf senescence in Arabidopsis

Previous studies have implicated *ELF4* in the regulation of leaf senescence, where mutants display early leaf-senescence phenotypes [26]. To investigate the roles of

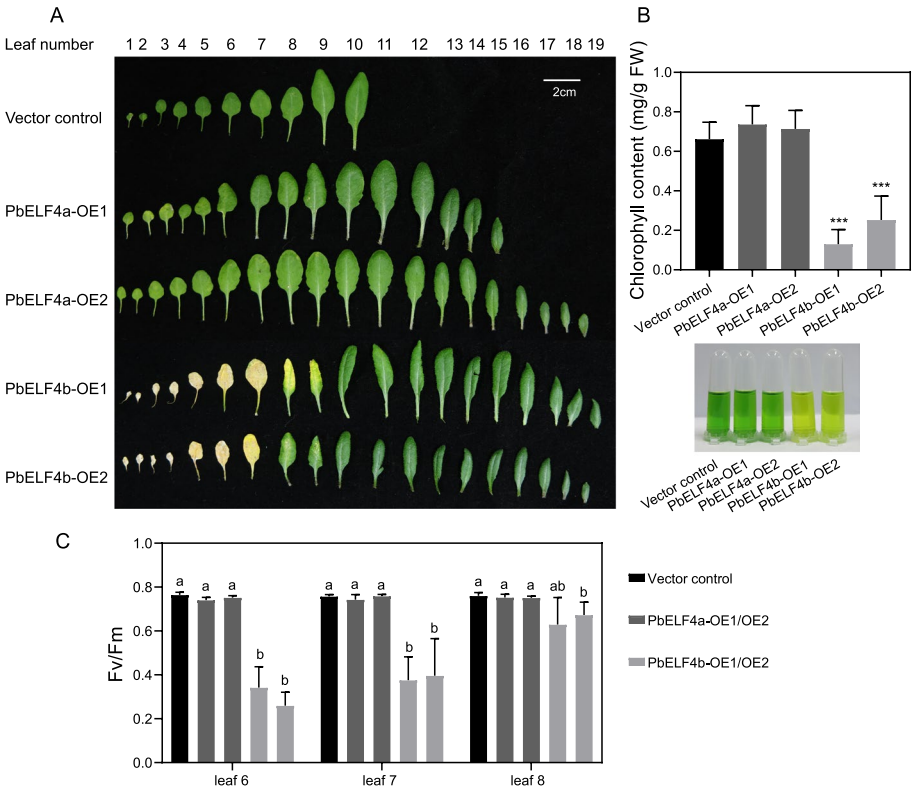


**Fig. 5** Senescent phenotypes induced by overexpression of *PbELF4a* and *PbELF4b* in Arabidopsis plants. **A** Representative rosette leaf phenotypes of vector control plants, PbELF4a-OE, and PbELF4b-OE transgenic lines grown under long-day conditions (16 h light/8 h dark) for 38 days. Scale bar = 2 cm. **B** Total chlorophyll content and the phenotype of leaves 6 to 8 in control plants and transgenic lines. Data are presented as means ± SD ($n = 4$). Statistical significance was determined using Student's *t*-tests compared to the vector control plants, *** indicates $P < 0.001$. **C** Fv (variable fluorescence)/Fm (maximal fluorescence) ratios of the 6$^{th}$, 7$^{th}$, and 8$^{th}$ leaves in control plants and transgenic lines. Data are presented as means ± SD ($n = 4$). Different letters indicate significant differences using one-way ANOVA Tukey's multiple range tests ($P < 0.05$)

*PbELF4a* and *PbELF4b* in leaf senescence, we observed the senescent phenotype of overexpression transgenic lines and vector control plants. Strikingly, while PbELF4a-OE transgenic lines exhibited leaf phenotypes similar to control plants, PbELF4b-OE transgenic lines displayed evident premature leaf yellowing (Fig. 5A). After 38 days of growth under long-day conditions (16 h light/8 h dark), the rosette leaves of control plants and PbELF4a-OE lines remained predominantly green. In contrast, the first to seventh rosette leaves of PbELF4b-OE lines showed pronounced yellowing, with the eighth rosette leaves beginning to exhibit signs of yellowing. To validate these observations, we measured the chlorophyll contents and chlorophyll fluorescence parameters (Fv/Fm). Consistently, the chlorophyll contents of the sixth to eighth leaves were substantially lower in PbELF4b-OE lines compared to those in control plants, whereas the difference between PbELF4a-OE lines and control plants was not significant (Fig. 5B). Similarly, the Fv/Fm values of these plants correlated with the observed leaf phenotypes (Fig. 5C).

Leaf senescence is a highly regulated process orchestrated by *SENESCENCE-ASSOCIATED GENES*. Numerous *SAGs* have been identified in Arabidopsis, including those encoding NAC transcription factors and chlorophyll degradation genes [30]. Compared to those in control plants, the expression levels of seven *NAC* genes were substantially upregulated in PbELF4b-OE lines (Fig. 6). Notably, *AtANAC019* and *AtANAC029* showed remarkable increases of 80-fold and 200-fold, respectively. While PbELF4a-OE lines did not exhibit significant phenotypic differences relative to control plants, the expression of *AtANAC059* and *AtANAC092* was downregulated in PbELF4a-OE lines. Moreover, the expression of *AtNYC1*, which encodes a chlorophyll b reductase, was substantially elevated in the leaves of PbELF4b-OE lines. These findings suggest that *PbELF4b* may promote leaf senescence and chlorophyll degradation.

### Subcellular localization of PbELF4a and PbELF4b

To determine the subcellular localization of PbELF4a and PbELF4b proteins, the coding sequences without

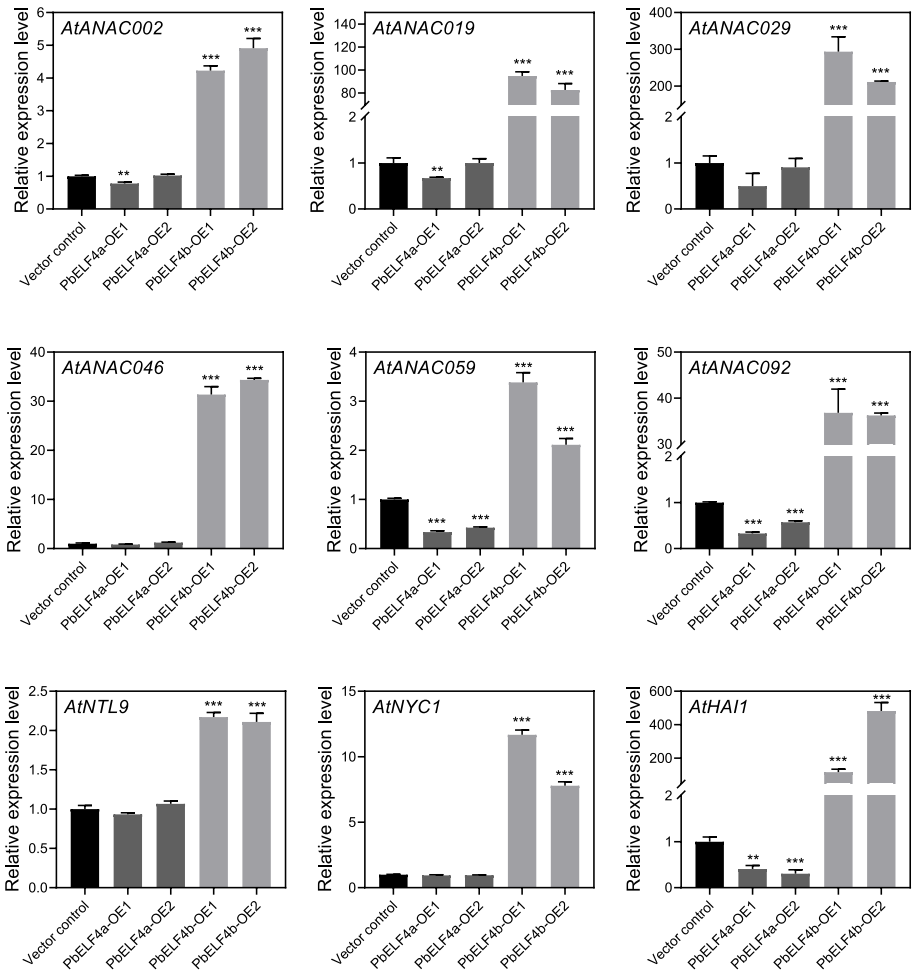


**Fig. 6** The expression levels of senescence-associated genes in the 8th leaves from 38-day-old vector control plants, PbELF4a-OE, and PbELF4b-OE transgenic lines are depicted. The expression of each gene in control plants was normalized to "1," with *AtACT* serving as the internal control. Data are presented as means ± SD ($n = 3$). Statistical significance was determined using Student's *t*-tests compared to the vector control plants, ** indicates $P < 0.01$, *** indicates $P < 0.001$

termination codons of the two genes were fused to a vector carrying the green fluorescent protein (GFP). The resulting recombined constructs were transiently expressed in tobacco leaves, and the fluorescence signals were visualized using laser scanning confocal microscopy. Both PbELF4a-GFP and PbELF4b-GFP fusion proteins exhibited signals specifically localized to the nucleus, as evidenced by their colocalization with DAPI, which stains nuclei. In contrast, the signal from the vector control was distributed throughout the cell (Fig. 7). These findings indicate that PbELF4a and PbELF4b were nuclear-localized proteins.

#### Interaction assay of PbELF4a and PbELF4b with PbELF3α

Previous studies on Arabidopsis have highlighted the pivotal role of the EC, which includes ELF4, in orchestrating various aspects of growth and development, such as flowering and leaf senescence [26, 41]. Within this complex, AtELF4 directly interacts with AtELF3 [9]. Hence, we aimed to study the interaction between PbELF4a/PbELF4b and PbELF3α from pear [37]. Initially, *PbELF4a* and *PbELF4b* were individually inserted into the pGADT7 vector, while *PbELF3α* was inserted into the pGBKT7 vector. The yeast two-hybrid assay revealed that yeast cells co-transformed with AD-PbELF4a and BD-PbELF3α displayed normal growth on SD/-Trp/-Leu/-His/-Ade medium. Conversely, yeast cells co-transformed with AD-PbELF4b and BD-PbELF3α failed to grow on the selective medium, suggesting that PbELF3α could interact with PbELF4a but not with PbELF4b (Fig. 8A and B). Subsequently, a firefly luciferase (LUC) complementation imaging assay was conducted in tobacco leaves to corroborate this interaction. Strong luminescence signal was observed in the area

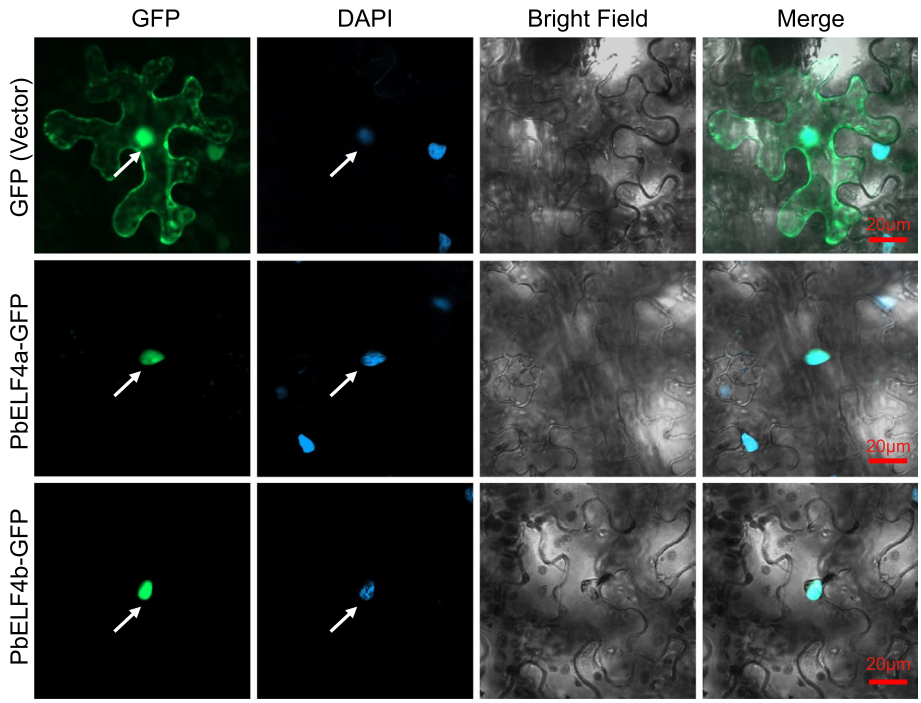


**Fig. 7** Subcellular localization of PbELF4a and PbELF4b proteins. The PbELF4a-GFP and PbELF4b-GFP fusion proteins, along with an empty vector as a control, were transiently expressed in tobacco leaf epidermal cells. The images were observed using confocal microscopy, with DAPI serving as a nuclear stain. Scale bars = 20 μm

co-expressing PbELF3α-nLUC and cLUC-PbELF4a, while no fluorescence signal was detected in the region co-expressing PbELF3α-nLUC and cLUC-PbELF4b (Fig. 8C and 8D). Collectively, these findings suggest that PbELF4a might participate in regulating plant flowering via a canonical pathway by interacting with PbELF3α, while PbELF4b may influence flowering and leaf senescence through alternative mechanisms.

## Discussion

Plant growth represents a dynamic continuum, wherein flowering and leaf senescence mark pivotal phases critical for plant productivity and breeding. The circadian clock serves as an endogenous regulatory mechanism that plants have evolved to synchronize numerous physiological processes in response to environmental cues during long-term adaptation. Extensive investigations have elucidated the functions of core clock genes across various species, encompassing roles in growth regulation, flowering, and stress response [32, 42, 43]. In pear, *PbLHY* and *PbELF3*, as homologs of clock genes in Arabidopsis, have been implicated in flowering regulation, while the potential contribution of *ELF4* in pear has remained elusive [37, 44]. This study presents a comprehensive analysis of five genes of the ELF4 family in pear, encompassing evolutionary relationships, sequence characteristics, and expression patterns. Moreover, the functional roles of two *PbELF4* genes exhibiting the highest *ELF4* homology were investigated, revealing the ability of *PbELF4a* and *PbELF4b* to impede flowering. Surprisingly, *PbELF4b* emerged as a contributor to the promotion of leaf senescence.

The ELF4 family is characterized by a conserved protein domain of unknown function (DUF1313) [7]. Homologous genes of *ELF4* have been identified across various species, including 3 in *Doritaenopsis* hybrid, 9 in soybean, and 21 in *Gossypium hirsutum* (cotton) [19, 22, 25]. The number of *ELF4* genes in pear (5) corresponds to that of Arabidopsis (5). Among these, PbELF4a and PbELF4b exhibit closer homology to AtELF4, while the remaining three cluster within the ELF4-like clade. Notably, *PbELF4a* and *PbELF4b* form a gene pair originating from dispersed duplication (DSD). DSD events involve unpredictable and random patterns, leading to the generation of gene copies that are neither located adjacent nor arranged collinearly [45], as observed in the majority of genes within the *Pinus tabuliformis* genome, contributing to enhanced adaptability [46]. Following gene duplication, expansion within gene families and functional divergence are common occurrences [47]. In pear, two *ELF4* gene pairs were derived from DSD, and three gene pairs were derived from WGD, while ELF4 family

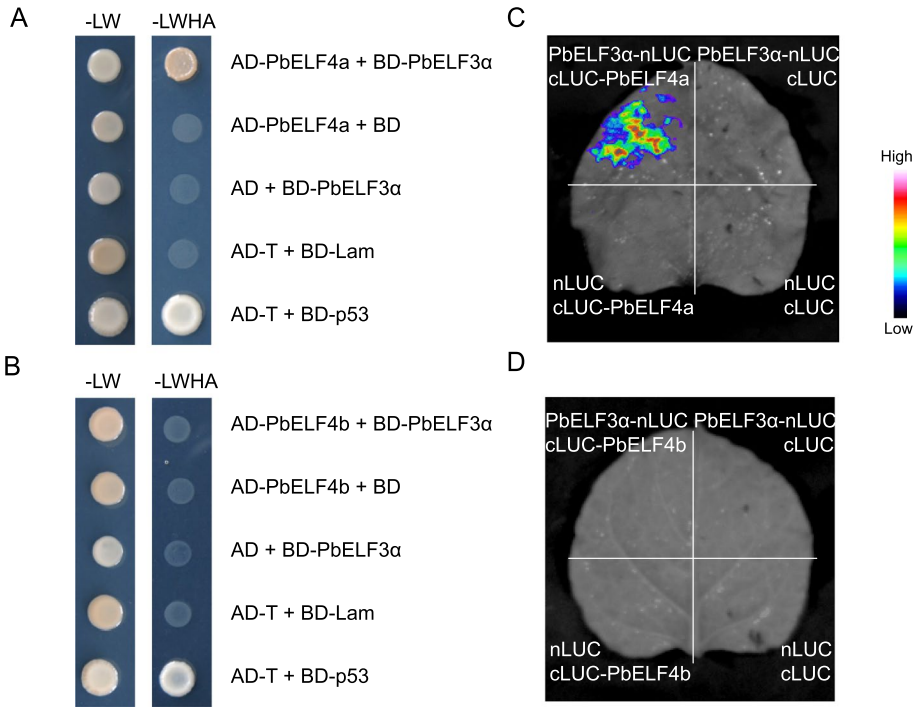


**Fig. 8** Verification of the interaction of PbELF4a and PbELF4b with PbELF3α proteins. (**A**) and (**B**) Yeast two-hybrid assays examining the interaction of PbELF4a and PbELF4b with PbELF3α proteins. Plasmid combinations were transferred into yeast strains, and interactions between prey and bait were tested on synthetic dropout (SD) media. SD-LW indicates SD media lacking Leu and Trp, while SD-LWHA indicates SD media lacking Leu, Trp, His, and Ade. (**C**) and (**D**) Firefly luciferase complementation imaging assays testing the interaction between PbELF4a and PbELF4b with PbELF3α proteins. *Agrobacterium* strain combinations were infected to the corresponding areas of tobacco leaves, with luminescence intensity depicted by the pseudo color bar

expansion in cotton is primarily attributed to segmental duplication [25]. This divergence in gene duplication mechanisms across species underscores the diverse strategies employed by the ELF4 family to adapt to varying environmental pressures.

*ELF4* genes exhibit wide expression across various growth stages and developmental phases in Arabidopsis [48]. Detailed studies in different leaf tissues have shown that *AtELF4* gene is expressed significantly higher in the vasculature than in mesophyll [49]. *GhELF4* genes in cotton are predominantly expressed in reproductive organs and leaves [25]. In *Doritaenopsis* hybrid, *DhEFL2*, *3* and *4* genes exhibit higher expression levels in stem, petal, and bud, respectively [19]. In this study, the expression patterns of *PbELF4* genes in pear tissues varied significantly. For instance, *PbELF4a* showed higher expression in leaf buds, whereas *PbELF4b* exhibited higher expression levels in stamen tissues. Additionally, *PbELF4a* and *PbELF4b* displayed contrasting expression trends throughout fruit development. These findings underscore the potential multifaceted biological roles of *PbELF4* genes across various stages of the pear life cycle. However, a comprehensive understanding of their biological functions requires further detailed exploration and verification.

As a fundamental component of circadian clock, *AtELF4* exhibits a strong diurnal expression rhythm [6]. In soybean and cotton, homologous *AtELF4* genes reach their peak expression in the evening [9, 22, 25]. The *PbELF4* genes in pear displayed diurnal expression rhythms similar to *AtELF4*, which were evident under a 12-h light/dark cycle as well as under both long- and short-day conditions. Plants utilize the circadian clock to sense photoperiods and regulate developmental transitions such as flowering, dormancy, and senescence [50, 51]. In this study, *PbELF4* genes showed obvious response to photoperiodic changes. Short-day conditions induced earlier peaks in the transcription of *PbELF4* genes. The input of external light signals affects the endogenous rhythms of clock-related genes. Daylength information controls the transcript patterns and protein accumulation of CO throughout the day by altering the peak time of clock-related genes. Under long-day conditions, the rhythmic synchronization of related genes ensures that CO activates the flowering at the appropriate time in Arabidopsis [51]. In the model tree *Populus* spp. (poplar), changes in daylength adjust the timing of the circadian clock to coordinate optimal times for vital processes [52]. Additionally, photoperiod regulates physiological

activities through homologous genes of circadian clock in pear [53]. Thus, *PbELF4* genes may play important roles in the photoperiod pathway.

*ELF4* was initially identified in genetic screening of photoperiodic mutants exhibiting a typical early-flowering phenotype [6]. The central regulatory gene *CO* integrates signals from the circadian clock and photoperiod to regulate flowering [4]. Notably, the expression of *CO* is increased in *elf4* mutants, indicating that the mechanism of *ELF4* influencing flowering is similar to that of other clock genes [6]. *AtEFL1* and *AtEFL3* inhibit flowering by reducing the expression of *AtCO* and *AtFT* [8]. Overexpression of *GmELF4* in Arabidopsis delays flowering and alters the expression of *AtCO* and *AtFT* [22], suggesting conservation in the mechanism of *ELF4*-mediated flowering regulation across different species. In this study, overexpression of *PbELF4a* and *PbELF4b* negatively regulated flowering through the same pathway. Moreover, as the scaffold protein of the evening complex, AtELF3 connects AtELF4 and AtLUX together, and AtELF4 influences the nuclear localization of AtELF3 [9, 54]. *ELF4* and *ELF3* have been shown to be closely related in several studies [41, 55]. *ELF3* has also been demonstrated to modulate flowering as a key repressor in various species [10, 11, 56, 57]. During the expansion of soybean from temperate to tropical regions and *Zea mays* (maize) from tropical to temperate regions, *ELF3* homologous genes and their complex (EC) regulate flowering [21, 58]. In maize, *ZmELF3.1* and *ZmELF4.1* display diurnal expression patterns under long- and short-day conditions. ZmELF3.1 also physically interacts with ZmELF4.1, and the *Zmelf3.1* mutants delay flowering [58]. *PbELF3α*, a homolog of *AtELF3*, has been associated with pear flower induction, and its overexpression in Arabidopsis leads to delayed flowering [37]. Subcellular localization studies have revealed that PbELF4a and PbELF4b are nuclear proteins, consistent with the localization of AtELF4 and PbELF3α [37, 54]. However, while PbELF3α was shown to directly interact with PbELF4a, no such interaction was observed with PbELF4b. Thus, we deduce that *PbELF4a* may regulate flowering in conjunction with *PbELF3α*, while the specific mechanism of *PbELF4b* remains to be explored further.

In addition to its well-established role in flowering, accumulating evidences suggest that the circadian clock regulates leaf senescence, with key genes such as *AtCCA1*, *AtPRR9*, *AtELF3*, and *AtELF4* having been preliminarily elucidated [26, 33, 34, 36]. Leaf senescence is a pivotal process throughout the entire plant growth and development cycle [59]. Chlorophyll degradation, a characteristic of leaf senescence, is accompanied by the activation of *SAGs* [28]. Before flowering in *PbELF4b* overexpression transgenic plants, early senescence was evident in rosette leaves, accompanied by a notable reduction in chlorophyll content compared to that in control plants. Meanwhile, the expression levels of several endogenous *SAGs*, including *AtANAC029*/*NAP*, *AtANAC046*, and *AtANAC092*/*ORE1*, were significantly upregulated. Senescence is orchestrated by an intricate regulatory network wherein families of transcription factors play pivotal roles [60, 61]. Among them, *NAC* genes act as central regulators, and the *NAC* genes identified in this study are all positive regulatory factors [29], suggesting that *PbELF4b* may promote leaf senescence. Different from *AtELF4* that delays senescence in Arabidopsis [26, 36], *PbELF4b* overexpression led to early senescence in leaves. The regulatory mechanism governing *PbELF4b*'s involvement in senescence warrants further investigation. Previous studies utilizing co-expression network analysis revealed that *PbELF4b* is closely associated with numerous plant hormone-related genes [53]. In cotton, *GhELF4* genes may be involved in the regulation of abscisic acid. Silencing of *GhELF4-1* and *GhEFL3-6* resulted in decreased stress resistance in cotton seedlings [25]. Given that *NAC* genes in Arabidopsis respond to hormones such as abscisic acid [29], it is conceivable that *PbELF4b* may operate within a similar pathway. It is found that for annual dynamic pattern, *PbELF4b* expressed higher in the early stage of leaf senescence in June and then decreased (Fig. S2). However, elucidating the relationship between *PbELF4b* and hormone signaling pathways requires future investigation.

## Conclusion

In this study, five *ELF4* homologous genes were identified in the pear genome. Comprehensive analyses, including assessments of phylogenetic relationships, conserved domains, gene structure, duplication events, and expression patterns, were conducted for all *PbELF4* genes. Our findings revealed that PbELF4a and PbELF4b proteins exhibit high homology with the AtELF4 protein and are localized in the nucleus. Notably, overexpression of *PbELF4a* and *PbELF4b* led to the inhibition of flowering in transgenic Arabidopsis plants, and *PbELF4b* overexpression further promoted leaf senescence. Interestingly, the flowering suppressor PbELF3α interacted with PbELF4a protein but not with PbELF4b protein, suggesting distinct regulatory pathways. Overall, our results shed light on the involvement of *PbELF4a* and *PbELF4b* in flowering regulation through diverse pathways, with *PbELF4b* emerging as a key gene in leaf senescence. These findings expand our understanding of clock-related genes in pear and provide valuable insights for further investigations into their functional roles.

## Materials and methods

### Plant materials and growth conditions

Various tissues and seeds of the pear cultivated variety "DangshanSuli" (*Pyrus bretschneideri*) were obtained

from germplasm resource nursery managed by the Pear Engineering Technology Research Center of Nanjing Agricultural University. Transcriptomic data for tissue-specific expression analysis were sourced from the online Pear Expression Database (http://www.peardb.org.cn/), which was released by our group. The detailed information of each tissue is described in the Plant materials section of the reference [40].

For diurnal expression analysis, pear seeds were stored in wet sand for two months, and the rooted seedlings were transferred to a culture room for 30 days to allow normal growth. The culture room was maintained at a temperature of 22 ℃, with a relative humidity of 65%, and a light intensity of 100 μmol $m^{-2}$ $s^{-1}$. The photoperiod was set to 12 h light/12 h dark, long-day conditions (16 h light/8 h dark) and short-day conditions (8 h light/16 h dark) respectively. The onset of light at the beginning of the photoperiod was defined as zeitgeber time zero (ZT0). Leaf samples from pear seedlings were collected at 4-h intervals starting from ZT1. Each biological replicate consisted of a mixture of leaves from three randomly selected pear seedlings. For annual dynamic expression analysis, leaf samples were collected from the 10-year-old pear trees on the 1st day of each month during May to December. Following collection, all samples were rapidly frozen in liquid nitrogen and stored at −80 ℃ until further experimentation.

*Arabidopsis thaliana* (Arabidopsis) and *Nicotiana tabacum* (tobacco) plants utilized in this study were cultivated in a suitable culture room. The photoperiod was set at 16 h light/8 h dark, while other growth conditions remained consistent with those described previously for the pear culture room.

#### Gene identification, phylogenetic relationship, and sequence feature analysis

To identify candidate ELF4/ELF4-like members in the pear genome, the protein sequences of five ELF4 members in Arabidopsis were subjected to a Base Local Alignment Search Tool (BLAST) search. The Arabidopsis sequences were obtained from the Arabidopsis Information Resource (http://www.Arabidopsis.org/) [62]. All pear protein and coding sequences were sourced from the DangshanSuli pear (*P. bretschneideri*) genome (https://gigadb.org/dataset/100083) [38].

To confirm PbELF4/ELF4-like members and analyze phylogenetic relationships, we utilized MEGA7 software for constructing a phylogenetic tree [63]. The parameters for the phylogenetic tree construction were set as follows: maximum likelihood method, JTT+G model, 1000 bootstrap replicates, and partial deletion. Protein sequences of reported species were obtained from various databases. PsELF4 in *Pisum sativum* (AAX47177.2) and DlELF4 in *Dimocarpus longan* (AHZ89708.1/ AIY68669.1) were retrieved from NCBI (https://www.ncbi.nlm.nih.gov/) [16, 18]. Protein sequences of other reported species, including GmELF4 in *Glycine max* (Glyma.18G027500), HaELF4-like in *Helianthus annuus* (ACK56112.1), CsELF4-like in *Citrus sinensis* (ACK56109.1), SlELF4-like in *Solanum lycopersicum* (ACK56116.1), BvELF4-like in *Beta vulgaris* (ACK56108.1), and DhELF4 in *Doritaenopsis* hybrid (AJR35694.1/AJR35695.1/AJD80258.1), were obtained from UniProt (https://www.uniprot.org/) [7, 19, 22].

Multiple sequences of PbELF4 and AtELF4 proteins were aligned using ClustalW and visualized with GeneDoc. The conserved domains of these proteins were analyzed using CD-search (https://www.ncbi.nlm.nih.gov/Structure/cdd/wrpsb.cgi) [64]. Structures of these genes were examined using the Gene Structure Display Server (http://gsds.gao-lab.org/) [65]. Duplication events of *PbELF4* genes were identified using the DupGen_finder pipeline as previously described [47]. Nonsynonymous substitution rates (Ka) and synonymous substitution rates (Ks) were calculated using KaKs_Calculator 2.0 with the Nei-Gojobori method [66].

#### RNA extraction and quantitative RT-PCR

Total RNA was extracted from pear leaves and Arabidopsis seedlings using a Plant Total RNA Isolation Kit Plus (FOREGENE, China) following the manufacturer's instructions. Subsequently, cDNA was synthesized using the One-Step gDNA Removal and cDNA Synthesis SuperMix (TransGen Biotech, China) according to the provided protocol. For quantitative RT-PCR analysis, specific primers targeting *PbELF4* genes were designed using Primer Premier 5.0 software (Table S3). The reference genes *PbUBQ* (*POLYUBIQUITIN*) for pear or *AtACT* (*ACTIN*) for Arabidopsis were utilized as internal controls to normalize gene expression levels. Quantitative RT-PCR was carried out using SYBR Green I Master Mix (Roche, Germany) on a Roche LightCycler 480 II instrument. Each sample was analyzed with three biological replicates, and relative expression levels were calculated using the $2^{-\Delta\Delta CT}$ method [67]. All experimental procedures adhered to the Minimum Information for Publication of Quantitative Real-Time PCR Experiments (MIQE) guidelines [68].

#### Subcellular localization and Arabidopsis plant transformation

The complete coding sequences of *PbELF4a* and *PbELF4b*, excluding the termination codon, were cloned by PCR. Subsequently, the corresponding products were cloned into the pCAMBIA1300-35S:CDS-GFP vector [69] using the ClonExpress II One Step Cloning Kit (Vazyme Biotech, China). Following confirmation by

sequencing, the fusion constructs (35S: PbELF4a-GFP and 35S: PbELF4b-GFP) along with the control plasmid (35S: GFP) were transformed into *Agrobacterium tumefaciens* strain GV3101. For subcellular localization analysis, the Agrobacterium solution was infiltrated into leaves of 4-week-old tobacco plants [70]. DAPI (Thermo Fisher Scientific, USA) staining was employed to visualize nuclei. The fluorescence signals in the transformed cells were observed using an LSM800 laser scanning confocal microscope (Zeiss, Germany).

For the Arabidopsis transformation assay, the above-mentioned strains were individually transformed into Arabidopsis (Columbia-0) using the floral dip method [71]. Positive transgenic plants were screened on Murashige and Skoog (MS) medium supplemented with hygromycin, and homozygous lines from the T3 generation were selected for subsequent experiments. Seeds were cultured on MS medium and vernalized at 4 ℃ for 3 days. Subsequently, the seeds were transferred to the culture room, and positive seedlings were transplanted into flowerpots after 10 days. The phenotypes of flowering and leaf senescence in transgenic plants were observed and analyzed. For gene expression analysis, 10-day-old seedlings and the eighth leaf of the 38-day-old plants were collected in the evening for RNA extraction.

### Measurements of chlorophyll content and chlorophyll fluorescence

For chlorophyll content measurement, leaves 6, 7, and 8 were weighed, ground, and then subjected to chlorophyll extraction in 95% (v/v) ethanol. The absorbance was determined at light wavelengths of 645 nm and 663 nm using a Spark multimode reader (TECAN, Switzerland). Total chlorophyll content was calculated as previously described [72]. For chlorophyll fluorescence measurement, the Fv (variable fluorescence)/Fm (maximal fluorescence) ratios of leaves 6, 7, and 8 were determined using an IMAGING-PAM system (Heinz Walz GmbH, Germany). Four biological replicates were included for each analysis.

### Yeast two-hybrid assay

The complete coding sequences of *PbELF4a* and *PbELF4b* were individually inserted into the pGADT7 vector while that of *PbELF3α* was inserted into the pGBKT7 vector. Following sequencing verification, various combinations of plasmids were transformed into the yeast strain AH109 using the lithium acetate (LiAC)-polyethylene glycol (PEG) method. Positive transformants were selected by growth on synthetic dropout (SD) medium lacking Leu and Trp (SD-LW). Protein interactions were subsequently screened on SD medium lacking Leu, Trp, His, and Ade (SD-LWHA). All yeast strains were incubated at 28 ℃ for 3–5 days to allow sufficient growth and interaction detection.

### Firefly luciferase complementation imaging assay

The complete coding sequences of *PbELF4a* and *PbELF4b* were individually inserted into the pCAMBIA1300-cLUC vector while that of *PbELF3α* was inserted into the pCAMBIA1300-nLUC vector. Following sequencing validation, the fusion constructs and control plasmids were separately transformed into *Agrobacterium tumefaciens* strain GV3101 carrying the pSoup vector. Tobacco leaves were then co-infiltrated with designated combinations of strains, and the infiltrated leaves were cultured under normal conditions for 2–3 days. Subsequently, D-luciferin potassium salt was sprayed onto the leaves, and luciferase activities were assessed using a plant living imaging system (Princeton Instruments, USA). The primers used for constructing the fusion constructs are listed in Table S3.

### Abbreviations

| | |
|---|---|
| ELF4 | EARLY FLOWERING 4 |
| CCA1 | CIRCADIAN CLOCK ASSOCIATED 1 |
| LHY | LATE ELONGATED HYPOCOTYL |
| PRR | PSEUDO RESPONSE REGULATOR |
| LUX | LUX ARRHYTHMO |
| EC | Evening complex |
| GI | GIGANTEA |
| CO | CONSTANS |
| FT | FLOWERING LOCUS T |
| SAG | SENESCENCE-ASSOCIATED GENE |
| NAC | NAM/ATAF/CUC |
| JA | Jasmonate |
| DSD | Dispersed duplication |
| WGD | Whole-genome duplication |
| DAF | Days after full bloom |
| ZT | Zeitgeber time |
| OE | Overexpression |
| GFP | Green fluorescent protein |
| LUC | Firefly luciferase |
| UBQ | POLYUBIQUITIN |
| ACT | ACTIN |
| qRT-PCR | Quantitative real-time PCR |

## Supplementary Information

The online version contains supplementary material available at https://doi.org/10.1186/s12870-024-05850-7.

Additional file 1. Fig. S1 Quantitative RT-PCR analysis of PbELF4a and PbELF4b expression in 10-day-old seedlings from control plants and transgenic lines. AtACT served as the internal control for gene expression analysis. Data are presented as means ± SD (n = 3). The sampling times were ZT1, ZT8, and ZT15.Fig. S2 Dynamic expression patterns of PbELF4a and PbELF4b during pear leaves development. The expression of PbELF4a in sample May was set to "1." PbUBQ was used as an internal control. Data are presented as means ± SD (n = 3).

Additional file 2. Table S1 Characteristics of ELF4 family members in pear and Arabidopsis.

Additional file 3. Table S2 Calculation of nonsynonymous substitution rates (Ka) and synonymous substitution rates (Ks) between PbELF4 gene pairs.

Additional file 4. Table S3 The Primers used in the assays.

**Acknowledgements**
We thank the Bioinformatics Center of Nanjing Agricultural University for supporting bioinformatic analysis. We thank Dr. Yuehua Ma (Central laboratory of College of Horticulture, Nanjing Agricultural University) for assistance in using laser scanning confocal microscope LSM800. We thank TopEdit (www.topeditsci.com) for its linguistic assistance during the preparation of this manuscript.

**Authors' contributions**
All authors contributed to the research planning and experimental designs; W.P., W.J.Y., Z.S.L. initiated and supervised the project; L.Z., L.W.J., W.Q., Q.K.J, X.Z.H. performed the experiments and analyzed the data; L.Z. and W.P. wrote the manuscript. All authors read and approved the final manuscript.

**Funding**
This work was supported by the National Natural Science Foundation of China (32302515, 32472687); Fundamental Research Program of Shanxi Province (20210302124231); Major Scientific and Technological Project of Xinjiang (2024A02006); the Fundamental Research Funds for the Central Universities (KJJQ2024013, RENCAI2024009); Xinjiang Forestry and Fruit Industry Research System (XJLGCYJSTX05-2024-07); Tianshan Talents Program of Xinjiang (2023D14015); Jiangsu Agricultural Science and Technology Innovation Fund (CX(24)1024); Priority Academic Program Development of Jiangsu Higher Education Institutions; and Earmarked Fund for China Agriculture Research System (CARS-28).

**Data availability**
The data generated and/or analyzed during the current study are available in the following repositories: The DangshanSuli pear (P. bretschneideri) genome is publicly available at GigaDB (https://gigadb.org/dataset/100083). Expression data is available at the Pear Expression Database (http://www.peardb.org.cn/). Other data used in this study are included in this article and the supplementary materials.
The DangshanSuli pear (*P. bretschneideri*) genome is publicly available at GigaDB (https://gigadb.org/dataset/100083). Expression data is available at the Pear Expression Database (http://www.peardb.org.cn/). Other data used in this study are included in this article and the supplementary materials.

## Declarations

**Ethics approval and consent to participate**
Not applicable.

**Consent for publication**
Not applicable.

**Competing interests**
The authors declare no competing interests.

Received: 15 August 2024 Accepted: 19 November 2024
Published online: 25 November 2024

**References**

1. Fornara F, de Montaigu A, Coupland G. SnapShot: Control of flowering in Arabidopsis. Cell. 2010;141(3):550 550 e551-552.
2. Blumel M, Dally N, Jung C. Flowering time regulation in crops-what did we learn from Arabidopsis? Curr Opin Biotechnol. 2015;32:121–9.
3. Song YH, Shim JS, Kinmonth-Schultz HA, Imaizumi T. Photoperiodic flowering: time measurement mechanisms in leaves. Annu Rev Plant Biol. 2015;66:441–64.
4. Shim JS, Kubota A, Imaizumi T. Circadian clock and photoperiodic flowering in Arabidopsis: CONSTANS is a hub for signal integration. Plant Physiol. 2017;173(1):5–15.
5. Nohales MA, Kay SA. Molecular mechanisms at the core of the plant circadian oscillator. Nat Struct Mol Biol. 2016;23(12):1061–9.
6. Doyle MR, Davis SJ, Bastow RM, McWatters HG, Kozma-Bognar L, Nagy F, et al. The ELF4 gene controls circadian rhythms and flowering time in Arabidopsis thaliana. Nature. 2002;419(6902):74–7.
7. Kolmos E, Nowak M, Werner M, Fischer K, Schwarz G, Mathews S, et al. Integrating ELF4 into the circadian system through combined structural and functional studies. HFSP J. 2009;3(5):350–66.
8. Lin K, Zhao H, Gan S, Li G. Arabidopsis ELF4-like proteins EFL1 and EFL3 influence flowering time. Gene. 2019;700:131–8.
9. Nusinow DA, Helfer A, Hamilton EE, King JJ, Imaizumi T, Schultz TF, et al. The ELF4-ELF3-LUX complex links the circadian clock to diurnal control of hypocotyl growth. Nature. 2011;475(7356):398–402.
10. Zagotta MT, Hicks KA, Jacobs CI, Young JC, Hangarter RP, Meeks-Wagner DR. The Arabidopsis ELF3 gene regulates vegetative photomorphogenesis and the photoperiodic induction of flowering. Plant J. 1996;10(4):691–702.
11. Hicks KA, Albertson TM, Wagner DR. EARLY FLOWERING3 encodes a novel protein that regulates circadian clock function and flowering in Arabidopsis. Plant Cell. 2001;13(6):1281–92.
12. Hazen SP, Schultz TF, Pruneda-Paz JL, Borevitz JO, Ecker JR, Kay SA. LUX ARRHYTHMO encodes a Myb domain protein essential for circadian rhythms. Proc Natl Acad Sci U S A. 2005;102(29):10387–92.
13. Ezer D, Jung JH, Lan H, Biswas S, Gregoire L, Box MS, et al. The evening complex coordinates environmental and endogenous signals in Arabidopsis. Nat Plants. 2017;3:17087.
14. Kim Y, Yeom M, Kim H, Lim J, Koo HJ, Hwang D, et al. GIGANTEA and EARLY FLOWERING 4 in Arabidopsis exhibit differential phase-specific genetic influences over a diurnal cycle. Mol Plant. 2012;5(3):678–87.
15. Kim Y, Lim J, Yeom M, Kim H, Kim J, Wang L, et al. ELF4 regulates GIGANTEA chromatin access through subnuclear sequestration. Cell Rep. 2013;3(3):671–7.
16. Liew LC, Hecht V, Laurie RE, Knowles CL, Vander Schoor JK, Macknight RC, et al. DIE NEUTRALIS and LATE BLOOMER 1 contribute to regulation of the pea circadian clock. Plant Cell. 2009;21(10):3198–211.
17. Jia T, Wei D, Meng S, Allan AC, Zeng L. Identification of regulatory genes implicated in continuous flowering of longan (Dimocarpus longan L.). PLoS One. 2014;9(12):e114568.
18. Fu Z, Jia T, Peng Y, Saquib W, Zeng L. Cloning and function analysis of ELF4 homolog genes in Dimocarpus longan. Acta Horticulturae Sinica. 2018;45:875–86.
19. Chen W, Qin Q, Zhang C, Zheng Y, Wang C, Zhou M, et al. DhEFL2, 3 and 4, the three EARLY FLOWERING4-like genes in a Doritaenopsis hybrid regulate floral transition. Plant Cell Rep. 2015;34(12):2027–41.
20. Lu S, Zhao X, Hu Y, Liu S, Nan H, Li X, et al. Natural variation at the soybean J locus improves adaptation to the tropics and enhances yield. Nat Genet. 2017;49(5):773–9.
21. Bu T, Lu S, Wang K, Dong L, Li S, Xie Q, et al. A critical role of the soybean evening complex in the control of photoperiod sensitivity and adaptation. Proc Natl Acad Sci U S A. 2021;118(8): e2010241118.
22. Marcolino-Gomes J, Nakayama TJ, Molinari HBC, Basso MF, Henning LMM, Fuganti-Pagliarini R, et al. Functional characterization of a putative Glycine max ELF4 in transgenic Arabidopsis and its role during flowering control. Front Plant Sci. 2017;8:618.
23. Chen WW, Takahashi N, Hirata Y, Ronald J, Porco S, Davis SJ, et al. A mobile ELF4 delivers circadian temperature information from shoots to roots. Nat Plants. 2020;6(4):416–26.
24. Khanna R, Kikis EA, Quail PH. EARLY FLOWERING 4 functions in phytochrome B-regulated seedling de-etiolation. Plant Physiol. 2003;133(4):1530–8.
25. Tian M, Wu A, Zhang M, Zhang J, Wei H, Yang X, et al. Genome-wide identification of the Early Flowering 4 (ELF4) gene family in cotton and silent GhELF4-1 and GhEFL3-6 decreased cotton stress resistance. Front Genet. 2021;12: 686852.
26. Zhang Y, Wang Y, Wei H, Li N, Tian W, Chong K, et al. Circadian evening complex represses jasmonate-induced leaf senescence in Arabidopsis. Mol Plant. 2018;11(2):326–37.
27. Guo Y, Ren G, Zhang K, Li Z, Miao Y, Guo H. Leaf senescence: progression, regulation, and application. Mol Hortic. 2021;1(1):5.
28. Lei P, Yu F, Liu X. Recent advances in cellular degradation and nuclear control of leaf senescence. J Exp Bot. 2023;74(18):5472–86.
29. Kim HJ, Nam HG, Lim PO. Regulatory network of NAC transcription factors in leaf senescence. Curr Opin Plant Biol. 2016;33:48–56.
30. Cao J, Zhang Y, Tan S, Yang Q, Wang HL, Xia X, et al. LSD 4.0: an improved database for comparative studies of leaf senescence. Mol Hortic. 2022;2(1):24.
31. Wang Y, Zhang Y, Wang L. Cross regulatory network between circadian clock and leaf senescence is emerging in higher plants. Front Plant Sci. 2018;9:700.
32. Lee J, Kang MH, Kim JY, Lim PO. The role of light and circadian clock in regulation of leaf senescence. Front Plant Sci. 2021;12: 669170.

33. Song Y, Jiang Y, Kuai B, Li L. CIRCADIAN CLOCK-ASSOCIATED 1 inhibits leaf senescence in Arabidopsis. Front Plant Sci. 2018;9:280.
34. Kim H, Kim HJ, Vu QT, Jung S, McClung CR, Hong S, et al. Circadian control of ORE1 by PRR9 positively regulates leaf senescence in Arabidopsis. Proc Natl Acad Sci U S A. 2018;115(33):8448–53.
35. Sakuraba Y, Jeong J, Kang MY, Kim J, Paek NC, Choi G. Phytochrome-interacting transcription factors PIF4 and PIF5 induce leaf senescence in Arabidopsis. Nat Commun. 2014;5:4636.
36. Kim H, Park SJ, Kim Y, Nam HG. Subcellular localization of GIGANTEA regulates the timing of leaf senescence and flowering in Arabidopsis. Front Plant Sci. 2020;11: 589707.
37. Wang P, Li Y, Liu Z, Li X, Wang Y, Liu W, et al. Reciprocal regulation of flower induction by ELF3alpha and ELF3beta generated via alternative promoter usage. Plant Cell. 2023;35(6):2095–113.
38. Wu J, Wang Z, Shi Z, Zhang S, Ming R, Zhu S, et al. The genome of the pear (Pyrus bretschneideri Rehd.). Genome Res. 2013;23(2):396–408.
39. Li J, Hu E, Chen X, Xu J, Lan H, Li C, et al. Evolution of DUF1313 family members across plant species and their association with maize photoperiod sensitivity. Genomics. 2016;107(5):199–207.
40. Wang P, Wu X, Shi Z, Tao S, Liu Z, Qi K, et al. A large-scale proteogenomic atlas of pear. Mol Plant. 2023;16(3):599–615.
41. Huang H, Nusinow DA. Into the evening: Complex interactions in the Arabidopsis circadian clock. Trends Genet. 2016;32(10):674–86.
42. Steed G, Ramirez DC, Hannah MA, Webb AAR. Chronoculture, harnessing the circadian clock to improve crop yield and sustainability. Science. 2021;372(6541):eabc9141.
43. Sanchez SE, Kay SA. The plant circadian clock: From a simple timekeeper to a complex developmental manager. Cold Spring Harb Perspect Biol. 2016;8(12): a027748.
44. Liu Z, Zhu X, Liu W, Qi K, Xie Z, Zhang S, et al. Characterization of the REVEILLE family in Rosaceae and role of PbLHY in flowering time regulation. BMC Genomics. 2023;24(1):49.
45. Ganko EW, Meyers BC, Vision TJ. Divergence in expression between duplicated genes in Arabidopsis. Mol Biol Evol. 2007;24(10):2298–309.
46. Niu S, Li J, Bo W, Yang W, Zuccolo A, Giacomello S, et al. The Chinese pine genome and methylome unveil key features of conifer evolution. Cell. 2022;185(1):204–17 e214.
47. Qiao X, Li Q, Yin H, Qi K, Li L, Wang R, et al. Gene duplication and evolution in recurring polyploidization-diploidization cycles in plants. Genome Biol. 2019;20(1):38.
48. Schmid M, Davison TS, Henz SR, Pape UJ, Demar M, Vingron M, et al. A gene expression map of Arabidopsis thaliana development. Nat Genet. 2005;37(5):501–6.
49. Endo M, Shimizu H, Nohales MA, Araki T, Kay SA. Tissue-specific clocks in Arabidopsis show asymmetric coupling. Nature. 2014;515(7527):419–22.
50. Singh RK, Svystun T, AlDahmash B, Jonsson AM, Bhalerao RP. Photoperiod- and temperature-mediated control of phenology in trees - a molecular perspective. New Phytol. 2017;213(2):511–24.
51. Johansson M, Staiger D. Time to flower: interplay between photoperiod and the circadian clock. J Exp Bot. 2015;66(3):719–30.
52. Singh RK, Bhalerao RP, Eriksson ME. Growing in time: exploring the molecular mechanisms of tree growth. Tree Physiol. 2021;41(4):657–78.
53. Liu Z, Liu W, Wang Z, Qi K, Xie Z, Zhang S, et al. Diurnal transcriptome dynamics reveal the photoperiod response of Pyrus. Physiol Plant. 2023;175(2): e13893.
54. Herrero E, Kolmos E, Bujdoso N, Yuan Y, Wang M, Berns MC, et al. EARLY FLOWERING4 recruitment of EARLY FLOWERING3 in the nucleus sustains the Arabidopsis circadian clock. Plant Cell. 2012;24(2):428–43.
55. Zhao H, Xu D, Tian T, Kong F, Lin K, Gan S, et al. Molecular and functional dissection of EARLY-FLOWERING 3 (ELF3) and ELF4 in Arabidopsis. Plant Sci. 2021;303: 110786.
56. Yoshida R, Fekih R, Fujiwara S, Oda A, Miyata K, Tomozoe Y, et al. Possible role of early flowering 3 (ELF3) in clock-dependent floral regulation by short vegetative phase (SVP) in Arabidopsis thaliana. New Phytol. 2009;182(4):838–50.
57. Ridge S, Deokar A, Lee R, Daba K, Macknight RC, Weller JL, et al. The chickpea Early Flowering 1 (Efl1) locus is an ortholog of Arabidopsis ELF3. Plant Physiol. 2017;175(2):802–15.
58. Zhao Y, Zhao B, Xie Y, Jia H, Li Y, Xu M, et al. The evening complex promotes maize flowering and adaptation to temperate regions. Plant Cell. 2023;35(1):369–89.
59. Zentgraf U, Andrade AG, Doll J. Editorial for special issue "Leaf Senescence" in plants. Plants (Basel). 2021;10(8):1490.
60. Zhang YM, Guo P, Xia X, Guo H, Li Z. Multiple layers of regulation on leaf senescence: New advances and perspectives. Front Plant Sci. 2021;12: 788996.
61. Woo HR, Kim HJ, Lim PO, Nam HG. Leaf senescence: Systems and dynamics aspects. Annu Rev Plant Biol. 2019;70:347–76.
62. Swarbreck D, Wilks C, Lamesch P, Berardini TZ, Garcia-Hernandez M, Foerster H, et al. The Arabidopsis Information Resource (TAIR): gene structure and function annotation. Nucleic Acids Res. 2008;36(Database issue):D1009-1014.
63. Kumar S, Stecher G, Tamura K. MEGA7: Molecular evolutionary genetics analysis version 7.0 for bigger datasets. Mol Biol Evol. 2016;33(7):1870–4.
64. Wang J, Chitsaz F, Derbyshire MK, Gonzales NR, Gwadz M, Lu S, et al. The conserved domain database in 2023. Nucleic Acids Res. 2023;51(D1):D384–8.
65. Hu B, Jin J, Guo AY, Zhang H, Luo J, Gao G. GSDS 2.0: an upgraded gene feature visualization server. Bioinformatics. 2015;31(8):1296–7.
66. Wang D, Zhang Y, Zhang Z, Zhu J, Yu J. KaKs_Calculator 2.0: a toolkit incorporating gamma-series methods and sliding window strategies. Genomics Proteomics Bioinformatics. 2010;8(1):77–80.
67. Livak KJ, Schmittgen TD. Analysis of relative gene expression data using real-time quantitative PCR and the 2(-Delta Delta C(T)) Method. Methods. 2001;25(4):402–8.
68. Bustin SA, Benes V, Garson JA, Hellemans J, Huggett J, Kubista M, et al. The MIQE guidelines: minimum information for publication of quantitative real-time PCR experiments. Clin Chem. 2009;55(4):611–22.
69. Xie Q, Wang P, Liu X, Yuan L, Wang L, Zhang C, et al. LNK1 and LNK2 are transcriptional coactivators in the Arabidopsis circadian oscillator. Plant Cell. 2014;26(7):2843–57.
70. Sparkes IA, Runions J, Kearns A, Hawes C. Rapid, transient expression of fluorescent fusion proteins in tobacco plants and generation of stably transformed plants. Nat Protoc. 2006;1(4):2019–25.
71. Clough SJ, Bent AF. Floral dip: a simplified method for Agrobacterium-mediated transformation of Arabidopsis thaliana. Plant J. 1998;16(6):735–43.
72. Jankovskis L, Kokina I, Plaksenkova I, Jermalonoka M. Impact of different nanoparticles on common wheat (Triticum aestivum L.) plants, course, and intensity of photosynthesis. ScientificWorldJournal. 2022;2022:3693869.


## Publisher's Note